A Constant ΔG Test for Measuring Mode I Interlaminar Fatigue Crack Growth Rates

by

A. J. Russell and K. N. Street

Defence Research Establishment Pacific
Victoria, BC, Canada

Paper presented at the Eighth ASTM Symposium on
Composite Materials: Testing and Design.
Charleston, SC. 29 April - 1 May 1986

ABSTRACT: A method for measuring Mode I interlaminar fatigue crack growth rates under constant strain energy release rate conditions is described and results are presented for two graphite fiber composite materials. The test consists of a uniform width and thickness DCB specimen which is loaded in series with a linear elastic spring in order to provide optimum control of ΔG. Tests are run under displacement control and delamination extension is determined by monitoring changes in compliance. A non-linear elastic relationship between load and displacement was required due to a non-linear material response caused by fiber bridging. Fatigue crack growth rates were observed to decline by as much as a factor of ten over a distance of less than 5 mm although this varied depending on material, lay-up and temperature. The fatigue crack growth behavior is compared with delamination extension under quasi-static loading and noticeable differences explained in terms of the micro-mechanisms responsible.

KEY WORDS: delamination, interlaminar fatigue, strain energy release rate, crack growth rate, fiber bridging, mode I, graphite/epoxy, thermoplastic, temperature, composite material

INTRODUCTION

It has now been well established by Russell and Street [1,2,3] and by de Charentenay et al [4,5] that one of the principle characteristics of Mode I delamination in many composite systems is the increase in fracture resistance which accompanies crack extension under quasi-static loading. This increase is less pronounced for unidirectional laminates than it is for angle-ply laminates and hence unidirectional specimens are preferable for test purposes in order to obtain conservative toughness values. The mechanism primarily responsible for this history-dependent behavior is the formation of a zone of fibers bridging the gap between the fracture faces directly behind the crack tip [1]. As the delamination extends, these bridged fibers gradually become strained and subsequently divert some of the available strain energy away from the crack tip.

During Mode I fatigue crack growth, a zone of bridged fibers also forms and, similarly, leads to an increase in fracture resistance. However, unlike the quasi-static case, it is more difficult to quantify the effects of this micro-failure mode on the crack growth rate (da/dN). The reason for this is that in most test specimens the strain energy release rate, G, changes as the crack extends and, hence, any decrease in da/dN due to fiber bridging is often obscured by the change due to ΔG.

For the frequently used double cantilever beam specimen (DCB) under constant amplitude, δ cycling, we have [6]

$$G \propto P^2 a^2 \propto \delta^2 / a^4 \qquad (1)$$

where P is the applied load and a is the crack length, and hence G decreases rapidly as the crack extends. Moreover, if a power law relationship exists between the fatigue crack growth rate and ΔG and has the form,

$$\frac{da}{dN} = B \cdot (\Delta G)^n \qquad (2)$$

where B and n are constants dependent on material, temperature, R ratio and frequency, then we can write,

$$\frac{da}{dN} \propto a^{-4n} \; . \qquad (3)$$

Therefore, since n is often greater than 5, a small increase in 'a' can result in a large reduction in da/dN particularly if 'a' is small. If tests are run under these conditions and fiber bridging develops gradually during the test, then the fatigue crack growth rate will drop off even faster than predicted by Equation 3 and 'n' will be overestimated. Indeed, values of n for high temperature graphite/epoxy obtained in this manner have been generally greater than 10 [7,8]. On the other hand, if tests were run under constant load cycling, the crack growth rate would increase as a^{2n} and if fiber bridging occurred, the increase would be reduced and 'n' would be underestimated. One method of overcoming this problem is to carry out testing under conditions of constant ΔG, then only da/dN need be monitored and plotted against crack length, 'a' for different values of ΔG.

A novel and simple method of carrying out such a test on uniform DCB specimens is described in this paper.

Fatigue crack growth under pure Mode I loading seldom occurs in composite structures. In general, both forward and anti-plane shear loading will be present in addition to tensile opening. However, a thorough understanding of the behavior of delaminations under each fracture mode alone is required before the factors affecting the numerous mode interactions can be determined and a predictive capability established. For Mode II delamination growth, either under quasi-static [2] conditions or in fatigue [3], no change in resistance is observed as the crack extends. However, for mixed-mode fracture, the behavior depends on the amount of Mode I present, with no change in resistance for 20 percent Mode I (CLS specimens) but with a large increase (even greater than for pure Mode I) occurring at 57 percent (MMF specimens) [2]. If only the fracture energies for <u>initiation</u> are considered, the situation is much simpler with G_c increasing linearly from G_{Ic} to G_{IIc} as the amount of shear increases [2]. Hence, it is probable also that the mixed-mode fatigue behavior will vary considerably depending on the ratio of fracture modes present. However, by considering only the initial values of fatigue crack growth rate, it may be possible again to make predictions on the basis of the pure Mode I and Mode II behaviors. This would provide designers with an upper limit on growth rates and also constitute a starting point from which the different loading mode/fiber bridging interactions could be evaluated.

EXPERIMENTAL ARRANGEMENT

Although several different experimental configurations would have achieved constant ΔG conditions, including both width and thickness tapered DCB specimens, the arrangement in Figure 1 was selected because of the ease of specimen fabrication and the well documented behavior of the uniform DCB specimen [6,9]. An elastic spring inserted in series with the specimen served to increase automatically the opening displacement of the specimen as the crack extended. By ensuring that the spring compliance was twice that of the initial specimen compliance, no immediate reduction in ΔG occurred and only after several millimeters of crack growth was it necessary to increase gradually the ram displacement in order to maintain ΔG constant. Delamination length was monitored by measuring the system compliance periodically. By selecting a relatively long initial crack length of 70 mm and by keeping the loading pins relatively close to the surface of the specimen, geometrically non-linear behavior was avoided. This ensured also that the shear displacement was negligible and allowed the use of the following beam theory expression for the compliance [7],

$$C_T = \frac{8a^3}{Ebh^3} + C_S = \frac{\delta_T}{P} \quad (= 1/k_1) \qquad (4)$$

where δ_T = total displacement
C_T = total compliance
C_S = spring compliance
E = flexural modulus
h = half thickness
b = width

It then follows that,

$$G = \frac{P^2}{2b} \cdot \frac{dC_T}{da} = \frac{3\delta_T{}^2 a^2 C_o}{2b a_o{}^3 C_T{}^2} \qquad (5)$$

where a_o = initial crack length
C_o = initial specimen compliance

and in order to maintain G or ΔG constant,

$$\delta_T = \delta_{To} \cdot \left[\frac{a_o C_T}{a(C_o + C_S)}\right] \qquad (6)$$

where δ_{To} = initial displacement.

Initial tests using these relationships were unsuccessful due to a material non-linearity which developed as the delamination grew. This took the form of a gradual loading of bridged fibers which resulted in an upward curvature of the load-displacement curves and had the effect of decreasing the measured compliance. As a consequence, Equation 4 was invalidated and significant errors were produced in calculating 'a' and G and in maintaining ΔG constant. However, supplementary tests on adhesively bonded graphite/epoxy specimens where fiber bridging did not occur proved that adequate control of ΔG was being achieved as shown by the linear increase in crack length in Figure 2.

In order to accommodate the effects of fiber bridging, an elastic but non-linear data reduction scheme was adopted. Experimentally, a second order relationship of the form,

$$P = k_1 \delta_T + k_2 \delta_T{}^2 \qquad (7)$$

was found to provide a good fit to the load-displacement data. Moreover, the linear stiffness term k_1 was equal to $1/C_T$ (as defined by Equation 4) thereby providing the required means of monitoring the delamination length. From the generalized definition of strain energy release rate [10],

$$G = -\frac{1}{b} \cdot \frac{dU}{da} \qquad (\delta \text{ constant}) \qquad (8)$$

where U = total elastic strain energy

and since from Equation 7,

$$U = \int P d\delta_T = \frac{k_1 \delta_T^{\,2}}{2} + \frac{k_2 \delta_T^{\,3}}{3} \qquad (9)$$

it follows that,

$$G = \frac{3\delta_T^{\,2} k_1^{\,2}}{2ba} \cdot \left[\frac{1}{k_1} - C_S \right] - \frac{\delta_T^{\,3}}{3b} \cdot \frac{dk_2}{da} \qquad (10)$$

and hence,

$$\delta_T = \delta_{To} \cdot \frac{k_{1o}}{k_1} \cdot \left[\frac{aC_o}{a_o(1/k_1 - C_S)} \right]^{0.5} + f(k_2, a) \qquad (11)$$

where $f(k_2,a)$ = function of k_2 and a to be determined by preliminary tests.

TEST PROCEDURE

Two different composite material systems were investigated; (1) A 177°C curing graphite/epoxy - AS1/3501-6 from Hercules and (2) A high temperature graphite/thermoplastic AS4/polyetherether ketone (PEEK) or APC2 from ICI.

Earlier static tests had shown that the effect of fiber bridging on the Mode I fracture energy of AS1/3501-6 laminates could be reduced by increasing the thickness of the interlaminar zone and by minimizing the amount of ply waviness. (See also Figure 8). In practise this could be achieved by reducing the extent of resin bleeding and by sandwiching the two center zero degree plys (which bounded the delamination) between two 90 degree plys. Therefore two different AS1/3501-6 laminates were fabricated, a $(0/90/0/90/0/90/0/90/0/90/0)_s$ lay-up with 55 percent average fiber volume fraction and a 24 ply unidirectional laminate with a fiber volume fraction of 65 percent. Only one laminate of AS4/PEEK was tested, a 3 mm thick unidirectional lay-up purchased directly from ICI. All laminates contained midplane implanted delamination starters, 0.025 mm thick, from which the fatigue cracks were grown. Specimens, 20 mm wide, were cut from the laminates with a diamond saw and kept in a dessicator until immediately prior to testing. Tests were run at 20 and 100 degrees Celsius and at ambient humidity.

Fatigue loading was carried out under stroke control in a 22 kN MTS load frame equipped with a 500 N load cell. Displacement was measured using the ram mounted LVDT since any errors due to the machine compliance were negligible compared to the much larger compliances of the specimen and spring. All tests were computer controlled and the data were stored automatically on magnetic disc for subsequent analysis. Fatigue tests on AS1/3501-6 were carried out at a frequency of 2.5 Hz whereas AS4/PEEK was tested at 1 Hz due to the latter's greater sensitivity to self heating. An R ratio of 0.05 was used for all tests.

Blocks of constant amplitude sinewave cycles were followed by slow ramp cycles having the same peak amplitude during which a minimum of 75 P,δ data pairs were measured. The values of k_1 and k_2 in Equation 7 were then evaluated by least squares fitting a second order curve to the data pairs. Any zero drift in either the load cell or LVDT was compensated for during each slow ramp cycle by completely unloading the specimen and re-determining the new load and displacement zero points. The load and displacement amplitudes were measured during the last 10 cycles of each block and used together with the new values of k_1 and k_2 to define the fatigue amplitude for the next block in accordance with Equation 11.

Following the completion of each test, the specimens were pulled apart and the initial and final crack lengths measured directly from visual observations of markings on the fracture surfaces. The k_1 values were then converted to crack lengths and values of da/dN calculated by fitting a smooth curve to the crack length versus number of cycles, N data. Next, the k_2 values were plotted against crack length and values of dk_2/da determined. Finally, ΔG values were calculated in accordance with Equation 10. In some cases, following fatigue the specimens were loaded to failure at 5 mm/min and the Mode I resistance to fracture, G_{IR}, calculated from Equation 10.

RESULTS

(a) Accuracy and Validity of Test

The single most important factor in the success of the test was the accuracy of measuring the delamination length since this affected not only da/dN but also ΔG and the ability to maintain ΔG constant. It was possible to compare the crack lengths predicted from the k_1 values with those measured directly from the specimen fracture surfaces at the end of each test since there was a visible difference in surface appearance between the fatigued and fractured parts of the specimen. Figure 3, which shows the correlation between predicted and measured values of 'a', indicates that for most tests the relationship between delamination length and k_1 as described in Equation 4 was valid.

Also of major importance in maintaining ΔG constant was the predictability of the dk_2/da term. Initial tests indicated that the non-linear stiffness k_2 increased at an approximately linear rate over the initial 10 to 20 mm of growth, as shown in Figure 4, and then either levelled off or declined. Since in most cases crack growth had virtually stopped after less than 10 mm, a constant value for dk_2/da was used in evaluating the fatigue amplitude for each block. However, in order for the non-linear contribution to the strain energy release rate in Equation 10 to vanish at $a=a_o$ it is necessary that $dk_2/da = 0$ initially. Hence the change in k_2 with 'a' shown as the solid line in Figure 4 was used to determine the fatigue amplitude for the next block. The

value of dk_2/da was determined by testing an initial specimen for each new set of experimental variables. Since the contribution to ΔG from the non-linear term was generally less than 12 percent of the total value this approximate correction method was acceptable. A representative example of the changes occurring in k_1, k_2, $\Delta\delta$ and ΔG during an actual test is shown in Figure 5.

(b) Material Behavior

For all specimens of both AS1/3501-6 and AS4/PEEK, the crack growth rate decreased as the crack extended. Several examples of this are shown in Figure 6 . In some tests run at high ΔG values and particularly for AS4/PEEK, the decrease in da/dN levelled off after 20 or 30 mm and a constant value of crack growth rate was achieved. This may also have occurred at lower ΔG values except that delamination growth became so slow that it was impractical to continue the tests. In addition to the decline in da/dN, a zone of bridged fibers was observed to form behind the advancing crack, Figure 7, and an increase in the Mode I fracture resistance occurred, Figure 8. Although this behavior was common to all specimens, the extent of fiber bridging and its effect on the crack growth rate was found to be dependent on material type, temperature, nature of the interlaminar zone and value of ΔG.

Figures 9, 10 and 11 contain plots of log(da/dN) versus log(ΔG) determined after different increments of crack growth. In Figure 9, the effects of lay-up and fiber volume fraction for AS1/3501-6 are shown. For ΔG values close to G_{Ic}, fatigue crack

growth rates were greater in the (90/0/0/90) lay-up. This was also true for lower ΔG values initially but as the delamination extended, da/dN fell more rapidly in the 90/0/0/90 laminate so that after 5 mm of crack growth there was little difference between them. The effect of raising the temperature on AS1/3501-6 was two-fold, as shown in Figure 10. First, it resulted in an increase in the da/dN values and second, it lowered the values of the ΔG exponent n. Figure 11 shows the da/dN vs ΔG values obtained for AS4/PEEK. Compared to the graphite/epoxy, the curves are shifted to higher ΔG values but have lower values of 'n'. In addition the curves corresponding to 0, 2 and 5 mm of crack growth are closer together than those for AS1/3501-6 indicating that the thermoplastic composite is less affected by fiber bridging. Also shown in Figure 10 is the da/dN vs. ΔG curve that is obtained if the spring is omitted and the fatigue amplitude is held constant. It is quite apparent that tests carried out in this manner underestimate the fatigue crack growth rates determined at low ΔG values and as a result yield too high a value of n.

DISCUSSION

The advantages of a constant ΔG test for measuring Mode I interlaminar fatigue crack growth rates are quite evident from the test results which show clearly the effects of the various test variables, as a function of both crack extension and strain energy release rate. Although fiber bridging operates during delamination extension under both static and fatigue conditions,

leading to many similarities in behavior, there are some major differences. Most noticeable is the fact that while the two AS1/3501-6 laminates have the same initial fracture energy (i.e. prior to fiber bridging), they do not have the same da/dN vs. ΔG curves corresponding to $\Delta a = 0$. One explanation is that unlike the initial fracture energy measurement which corresponds to incipient delamination extension, da/dN is determined after crack growth has taken place and hence includes the effects of fiber bridging and other possible crack blunting mechanisms sensitive to the nature of the interlaminar zone. It is also possible that da/dN falls off so rapidly during the first few tens of cycles that the first measurement of crack extension, normally made after a few hundred cycles, fails to yield the initial maximum value of da/dN.

Another surprising difference in laminate behavior is the rapid drop off in fatigue crack growth rate experienced by the 90/0/0/90 laminate at low values of ΔG compared to higher ΔG values (or quasi-static behavior) where the effects of fiber bridging are minimized. A microscopic examination of the fatigue surfaces, Figure 12, revealed that there were indeed fewer fibers appearing at the surface in the 90/0/0/90 specimens compared to the closely nested plys of the unidirectional laminate. However, where fiber bridging had occurred the fibers were deeply embedded in a layer of resin. Thus, a possible explanation of the observed behavior is that although there are likely to be fewer bridged fibers in the 90/0/0/90 laminate, where they do occur they require more energy to peel them from the surface. At low ΔG there is

insufficient crack opening to either peel or fracture the bridged fibers which therefore remain and divert strain energy from the crack tip. Under quasi-static extension or if ΔG is close to G_{Ic}, then fiber fracture occurs in preference to peel and the bridged fibers are eliminated. On the other hand, in the unidirectional laminate there will be many more bridged fibers but they will be peeled relatively easily from the surface allowing them to persist but reducing their capacity to divert strain energy from the advancing crack tip. This explanation is also consistent with the observation that during quasi-static growth, the 90/0/0/90 laminate undergoes slip/stick behavior (corresponding to alternating fiber bridging and bridged fiber fracture followed by a jump in crack length) whereas delamination extension in unidirectional laminates of AS1/3501-6 is always stable.

The increase in fatigue crack growth rate with temperature for AS1/3501-6 is consistent with a corresponding decrease in fracture energy [2] and the reduction in slope is also in agreement with the observation that as the matrix hardness is reduced so too is the value of n [3]. It is likely that hot/dry conditions are worst case for the Mode I fatigue of this material since the addition of absorbed moisture increases G_{Ic} and initial results indicate that it reduces the initial values of da/dN.

Figure 13 shows the da/dN vs. ΔG curves for AS1/3501-6 corresponding to $\Delta a = 0$ normalised to G_{Ic} as well as the final values of da/dN plotted against $\Delta G/G_{IR}$ where G_{IR} is the mode I fracture resistance measured from the end of the fatigue crack. For each of the two different laminates both the initial and final

da/dN points fall on the same line indicating that there is a single relationship between crack growth rate and fracture resistance, namely

$$\frac{da}{dN} = \left[\frac{\Delta G}{G_{IR}}\right]^n \qquad (12)$$

where G_{IR} = the instantaneous resistance to fracture.

A similar relationship was found for fatigue growth of edge delaminations [11], although the mechanism responsible for increasing fatigue resistance was matrix micro-cracking [12] and not fiber bridging. Furthermore, ΔG was normalised to the fracture resistance measured after an equal amount of quasi-static edge delamination. Such a normalisation would be invalid in the present case as the results of Figure 8 show that the fracture resistance following fatigue is significantly different from that following static growth and that it also depends on the value of ΔG.

A comparison of the normalised Mode I crack growth rate curves with Mode II data obtained at similar R ratios [3] indicates that for AS1/3501-6 at 20°C, Figure 13, the exponent n is greater in Mode I. In addition, the curve appears to be displaced to lower values of da/dN. Thus, unlike Mode II, delamination fatigue crack growth in Mode I is not a significant problem unless $\Delta G/G_{Ic} > 0.5$. On the other hand, for AS4/PEEK, Figure 14, both the Mode I and Mode II slopes are similar and although the Mode I curve is shifted to lower da/dN values, significant fatigue crack growth will occur if $\Delta G/G_{Ic} > 0.1$. Hence, from a design viewpoint Mode I delamination growth in

AS1/3501-6 is a static problem whereas in AS4/PEEK it is also a fatigue problem, and structural components may have to be designed to have a finite lifetime thereby losing some of the advantages of the substantially greater Mode I toughness.

CONCLUSIONS

Based on the experimental results the following conclusions can be made concerning the test method and the Mode I interlaminar fatigue crack growth behavior of the test materials.

(1) A novel and simple technique involving an elastic spring in series with a uniform DCB specimen allows Mode I delamination fatigue growth rate data to be obtained under conditions of constant strain energy release rate ΔG. This is of particular importance to materials such as graphite/epoxy which experience a large change in fracture resistance G_{IR} due to fiber bridging during delamination extension. Unless taken into account, such changes may lead to non-conservative values of the fatigue sensitivity of composite materials.

(2) Fiber bridging effects in Mode I delamination fatigue crack growth can reduce da/dN values by more than an order of magnitude. Their origin is closely related to manufacturing techniques and laminate lay-up geometries through the extent to which fiber (or bundle) nesting between adjacent plies takes place. Although it is unwise to rely on fiber bridging for design purposes, if

present it will provide an additional material safety factor.

(3) Based on initial values of fatigue crack growth rate where fiber bridging effects are minimized the following Mode I growth rate laws have been established for design purposes.

For AS1/3501-6 at f = 2.5 Hz and R = 0.05 and with G in J/m^2,

$$20^{o}C/dry,\ da/dn = 2.1x10^{-21}x(\Delta G)^{9.4}\ mm/cycle.$$

$$100^{o}C/dry,\ da/dN = 2.7x10^{-16}x(\Delta G)^{6.8}\ mm/cycle.$$

And for AS4/PEEK at f = 1.0 Hz and R = 0.05 and with G in J/m^2,

$$20^{o}C/dry,\ da/dN = 4.4x10^{-13}x(\Delta G)^{3.0}\ mm/cycle.$$

(4) Mode I delamination fatigue growth rates at $100^{o}C$ are approximately an order of magnitude greater than those at $20^{o}C$ for graphite/epoxy in the dry state. Hence the former constitutes at present a more useful "worst case" for design and damage tolerance analyses.

(5) For graphite/epoxy, fatigue sensitivity in Mode I is considerably lower than that in Mode II shear. However, for AS4/PEEK material, both Mode I and Mode II are characterized by significant delamination fatigue growth rates at low ratios of $\Delta G/G_c$. In addition, the favorable effects of fiber bridging are much less pronounced in the PEEK matrix system.

Acknowledgments

This work is part of the program in support of the Department of National Defence data base requirements for damage tolerance analyses of advanced materials in high performance aircraft. The authors are grateful to E. Jensen for conscientious assistance in the preparation and fabrication of test specimens as well as scanning electron microscope examinations.

REFERENCES

[1] Russell,A.J. and Street, K. N., "Factors Affecting the Interlaminar Fracture Energy of Graphite/Epoxy Laminates," in Progress in Science and Engineering of Composites, Proc. ICCM IV, T. Hayashi, K. Kawata and S. Umekawa Eds., Japan Society for Composite Materials, 1982, pp 279-286.

[2] Russell, A.J. and Street, K.N., "Moisture and Temperature Effects on the Mixed-Mode Delamination Fracture of Unidirectional Graphite/Epoxy," in Delamination and Debonding of Materials, ASTM STP 876, W. S. Johnson, Ed., American Society for Testing Materials, Philadelphia, 1985, pp 349-370.

[3] Russell, A. J. and Street, K. N., "The Effect of Matrix Toughness on Delamination: Static and Fatigue Fracture under Mode II Shear Loading of Graphite Fiber Composites," in Toughened Composites, ASTM STP XXX, N. J. Johnston, Ed., American Society for Testing Materials, Philadelphia, 1986, (in press)

[4] De Charentenay, F. X. and Benzeggagh, M., "Fracture Mechanics of Mode I Delamination in Composite Materials," Advances in Composite Materials, Proc. ICCM III, A. R. Bunsell et al Eds, Pergamon Press, 1980, pp 186-197.

[5] De Charentenay, F. X., Harry, J.M., Prel, Y. and Benzeggagh, M. L., "Characterizing the Effect of Delamination Defect by Mode I Delamination Test," in Effects of Defects in Composite Materials, ASTM STP 836, American Society for Testing Materials, 1984, pp 84-103.

[6] Gillis, P. P. and Gilman, J. J., "Double Cantilever Cleavage Mode of Crack Propagation," J. of Applied Physics, Vol 35, 1964, pp 647-658.

[7] Wilkins, D. J., Eisenmann, J. R., Camin, R. A., Margolis, W. S. and Benson, R. A., "Characterizing Delamination Growth in Graphite-Epoxy," in Damage in Composite Materials, ASTM STP 775, American Society for Testing Materials, Philadelphia, 1982, pp168-183.

[8] Ramkumar, R. L. and Whitcomb, J. D., "Characterization of Mode I and Mixed-Mode Delamination Growth in T300/5208 Graphite/Epoxy," in Delamination and Debonding of Materials, ASTM STP 876, W. S. Johnson, Ed., American Society for Testing and Materials, Philadelphia, 1985, pp. 315-335

[9] Mostovoy, S., Crosley, P. B. and Ripling, E. J., "Use of Crack-Line-Loaded Specimens for Measuring Plane-Strain Fracture Toughness," J. of Materials, Vol. 2, 1967, pp 661-681.

[10] Irwin, G. R. and de Wit, R., "A Summary of Fracture Mechanics Concepts," Journal of Testing and Evaluation, JTEVA, Vol. 11, Jan 1983, pp 56-65.

[11] Poursartip, A., "The Characterization of Delamination Growth in Laminates under Fatigue Loading," in Toughened Composites, ASTM STP XXX, N. J. Johnston, Ed., American Society for Testing Materials, Philadelphia, 1986, (in press)

[12] O'Brien, T. K., "Characterization of Delamination Onset and Growth in a Composite Laminate," in Damage in Composite Materials, ASTM STP 775, American Society for Testing and Materials, 1982, pp 140-167.

FIGURE CAPTIONS

1. Experimental arrangement for constant ΔG interlaminar fatigue.

2. Mode I fatigue crack growth versus number of cycles for EA-9321 bonded AS4/3501-6 graphite epoxy. $\Delta G = 278$ J/m^2.

3. Comparison of predicted versus measured values of final crack length after fatigue.

4. Example of increase in non-linear stiffness, k_2 with crack growth. The solid line indicates the k_2 behavior assumed at the start of the test in order to maintain ΔG constant.

5. Typical test results showing changes in linear and non-linear stiffnesses, k_1 and k_2, the corrections made to δ in order to maintain ΔG constant and the increase in delamination length a.

6. Representative plots of crack length versus number of cycles showing reduction in crack growth rates with delamination extension.

7. Photo showing extent of fiber bridging behind crack tip in AS1/3501-6 during fatigue.

8. Mode I fracture resistance values of AS1/3501-6 following fatigue crack growth. The numbers beside the data points are ΔG values in J/m^2.

9. Effect of lay-up and fiber volume fraction on the Mode I fatigue crack growth rate of AS1/3501-6.

10. Effect of temperature on the Mode I fatigue crack growth rate of AS1/3501-6.

11 Mode I fatigue crack growth behavior of AS4/PEEK.

12. Representative fracture surfaces of Mode I fatigued specimens.

13. Mode I fatigue crack growth rate of AS1/3501-6 normalised to fracture resistance or fracture energy. Dashed curve shows pure Mode II behavior from [3] for comparison.

14. Mode I fatigue crack growth rate of AS4/PEEK normalised to fracture energy. Dashed curve shows pure Mode II behavior from [3] for comparison. NB. The laminate from which the Mode I specimens were taken had a greater toughness than the Mode II laminate.

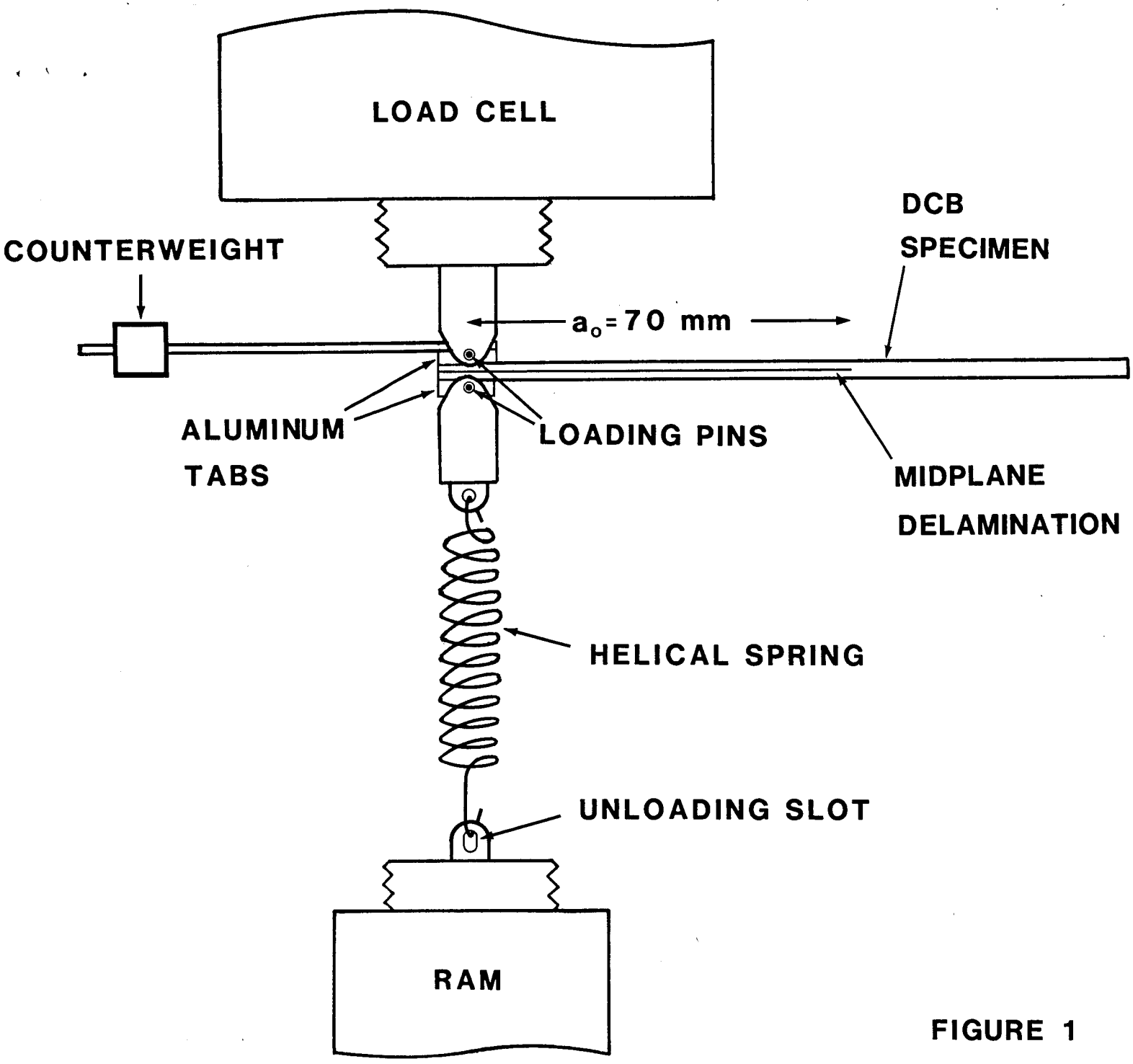
LOAD CELL
COUNTERWEIGHT
DCB
SPECIMEN
a_o = 70 mm
ALUMINUM
TABS
LOADING PINS
MIDPLANE
DELAMINATION
HELICAL SPRING
UNLOADING SLOT
RAM

FIGURE 1

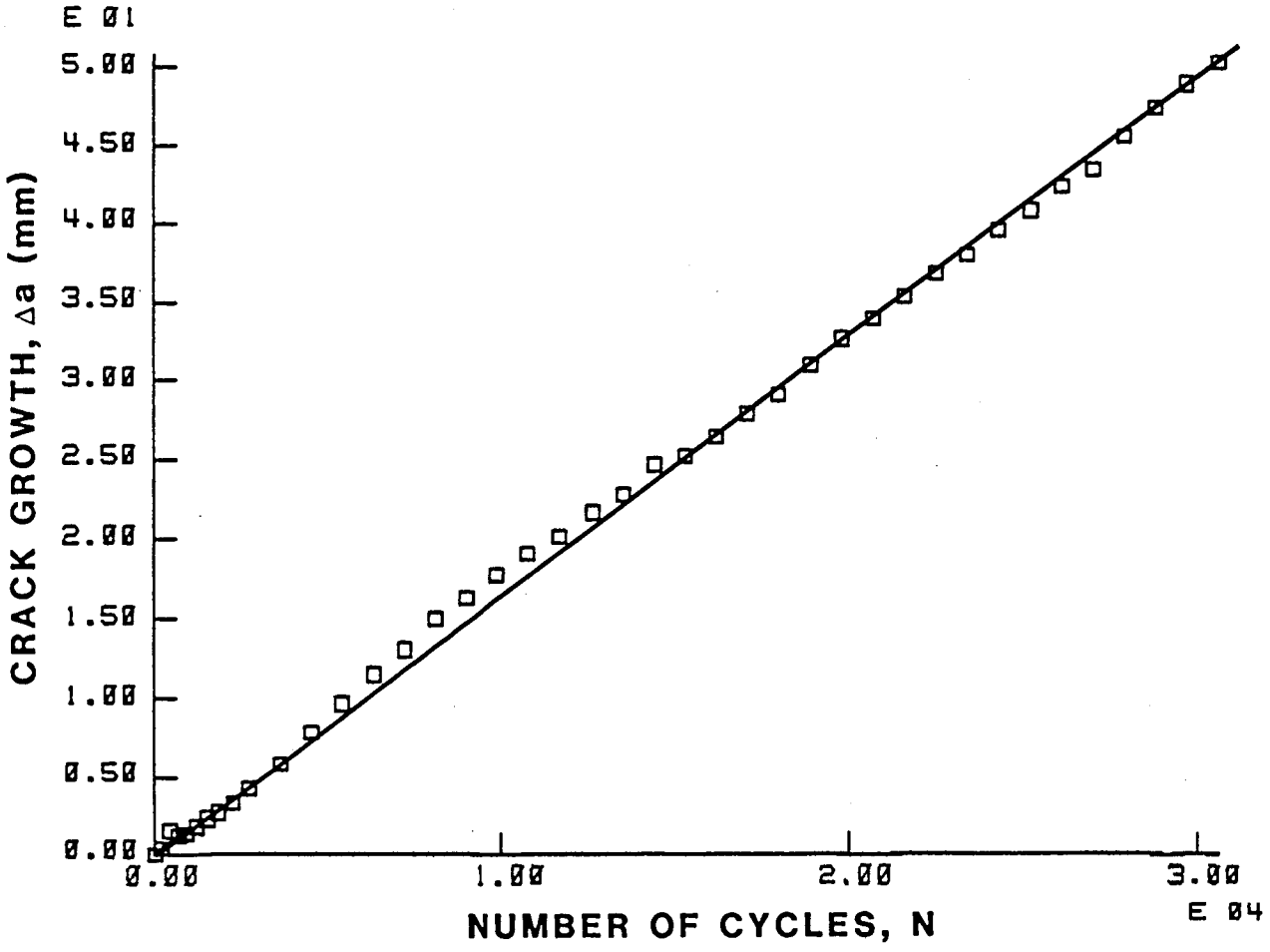
E 01
5.00
4.50
4.00
3.50
3.00
2.50
2.00
1.50
1.00
0.50
0.00
CRACK GROWTH, Δa (mm)
0.00
1.00
2.00
3.00
E 04
NUMBER OF CYCLES, N

FIGURE 2

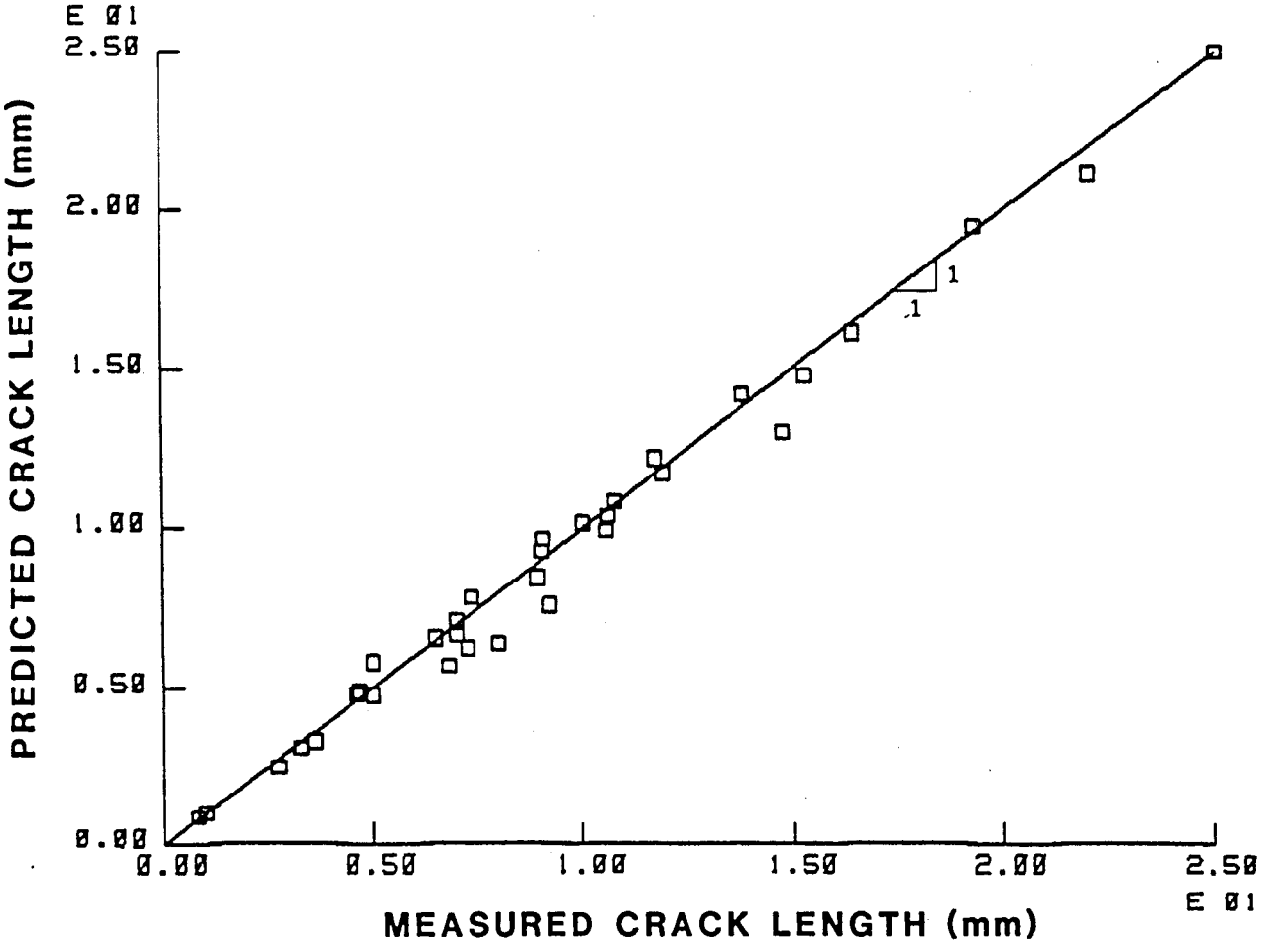
E 01
2.50
2.00
1.50
1.00
0.50
0.00
PREDICTED CRACK LENGTH (mm)
0.00
0.50
1.00
1.50
2.00
2.50
E 01
MEASURED CRACK LENGTH (mm)
1
1

FIGURE 3

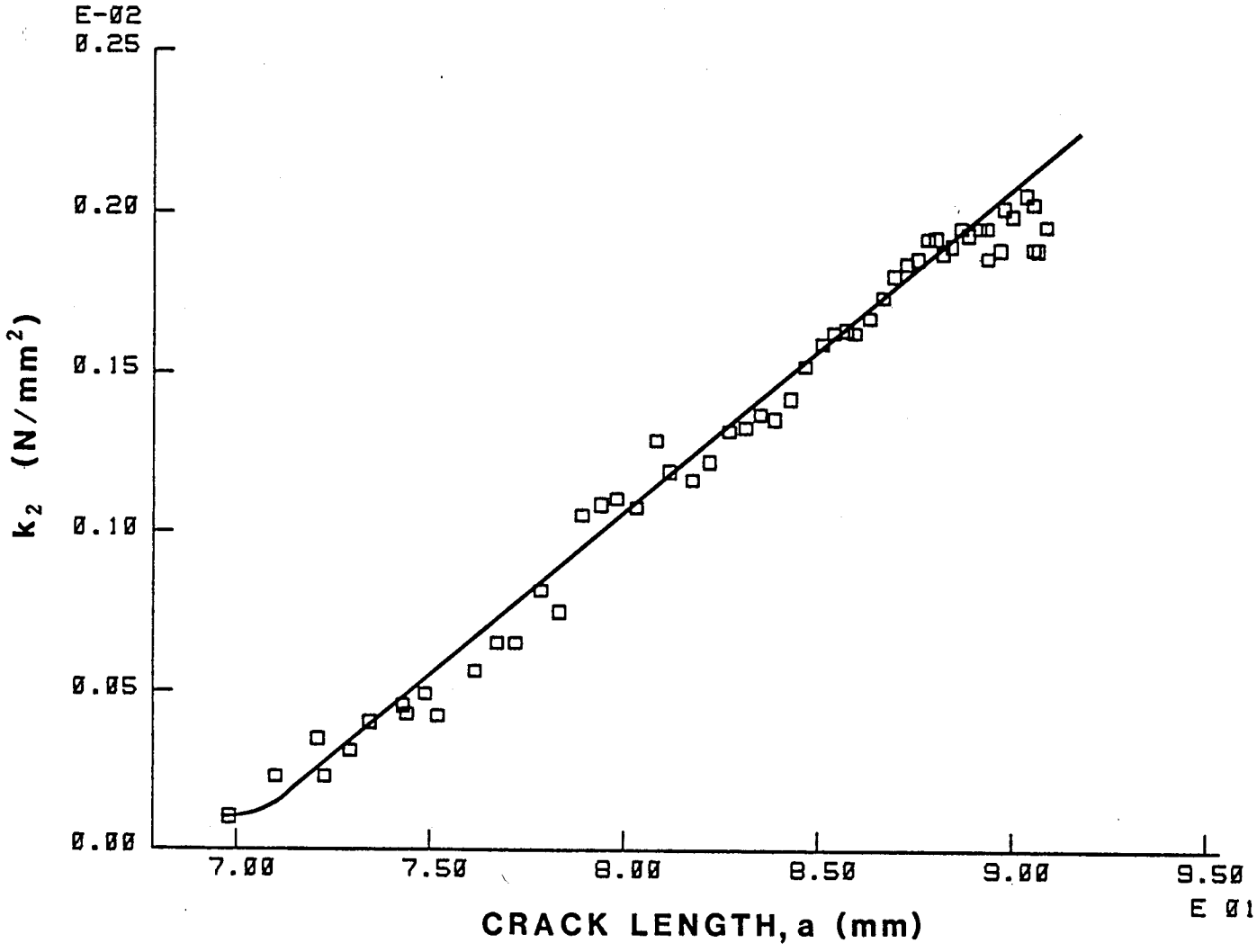
E-02
0.25
0.20
0.15
0.10
0.05
0.00
k_2 (N/mm^2)
7.00
7.50
8.00
8.50
9.00
9.50
E 01
CRACK LENGTH, a (mm)

FIGURE 4

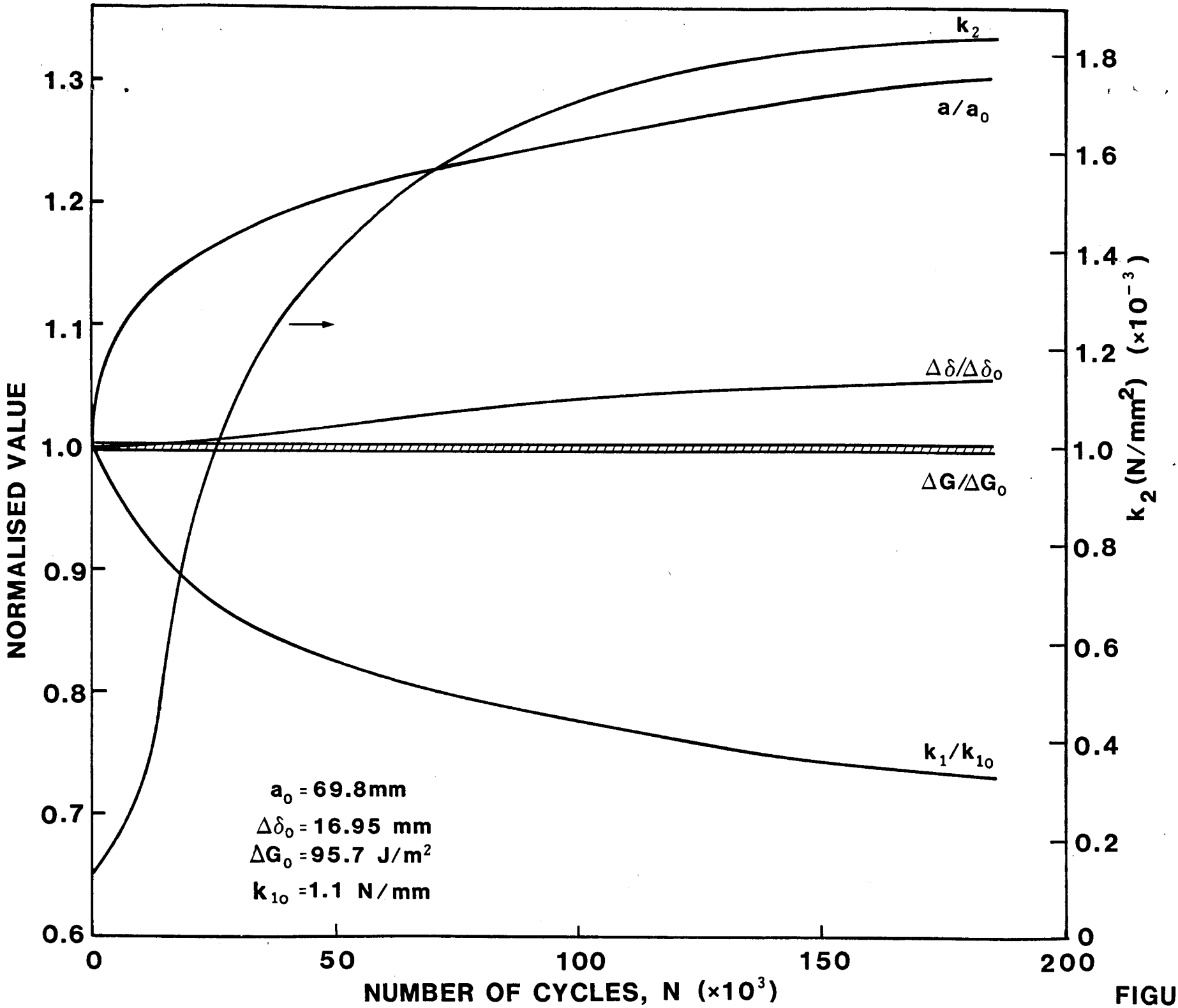
k_2
a/a_0
$\Delta\delta/\Delta\delta_0$
$\Delta G/\Delta G_0$
k_1/k_{1o}
$a_0 = 69.8mm$
$\Delta\delta_0 = 16.95$ mm
$\Delta G_0 = 95.7$ J/m^2
$k_{1o} = 1.1$ N/mm
NORMALISED VALUE
k_2 (N/mm^2) (×10^{-3})
NUMBER OF CYCLES, N (×10^3)
0.6
0.7
0.8
0.9
1.0
1.1
1.2
1.3
0
0.2
0.4
0.6
0.8
1.0
1.2
1.4
1.6
1.8
0
50
100
150
200

FIGURE 5

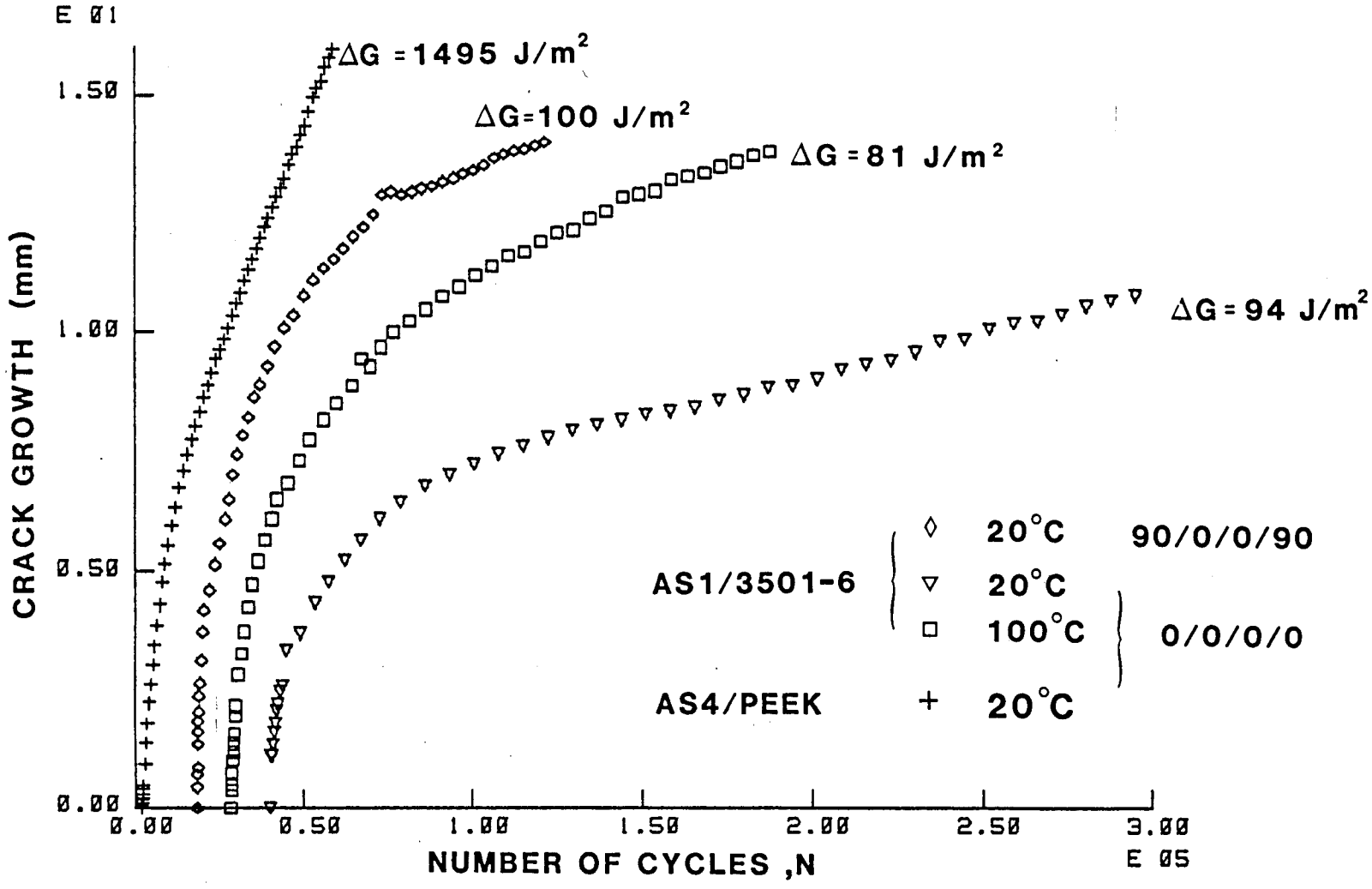
E 01
1.50
1.00
0.50
0.00
CRACK GROWTH (mm)
ΔG = 1495 J/m²
ΔG=100 J/m²
ΔG = 81 J/m²
ΔG = 94 J/m²
AS1/3501-6
20°C
90/0/0/90
20°C
100°C
0/0/0/0
AS4/PEEK
20°C
0.00
0.50
1.00
1.50
2.00
2.50
3.00
E 05
NUMBER OF CYCLES ,N

FIGURE 6

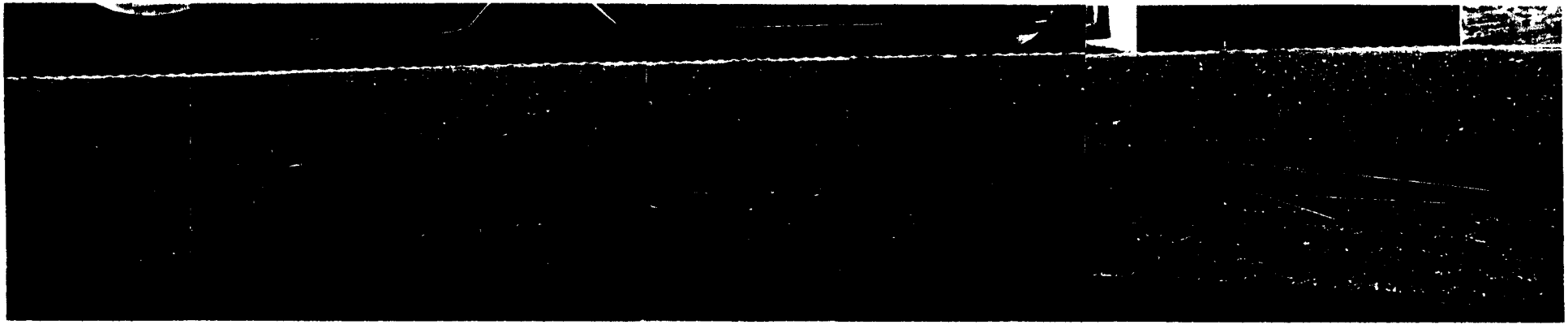

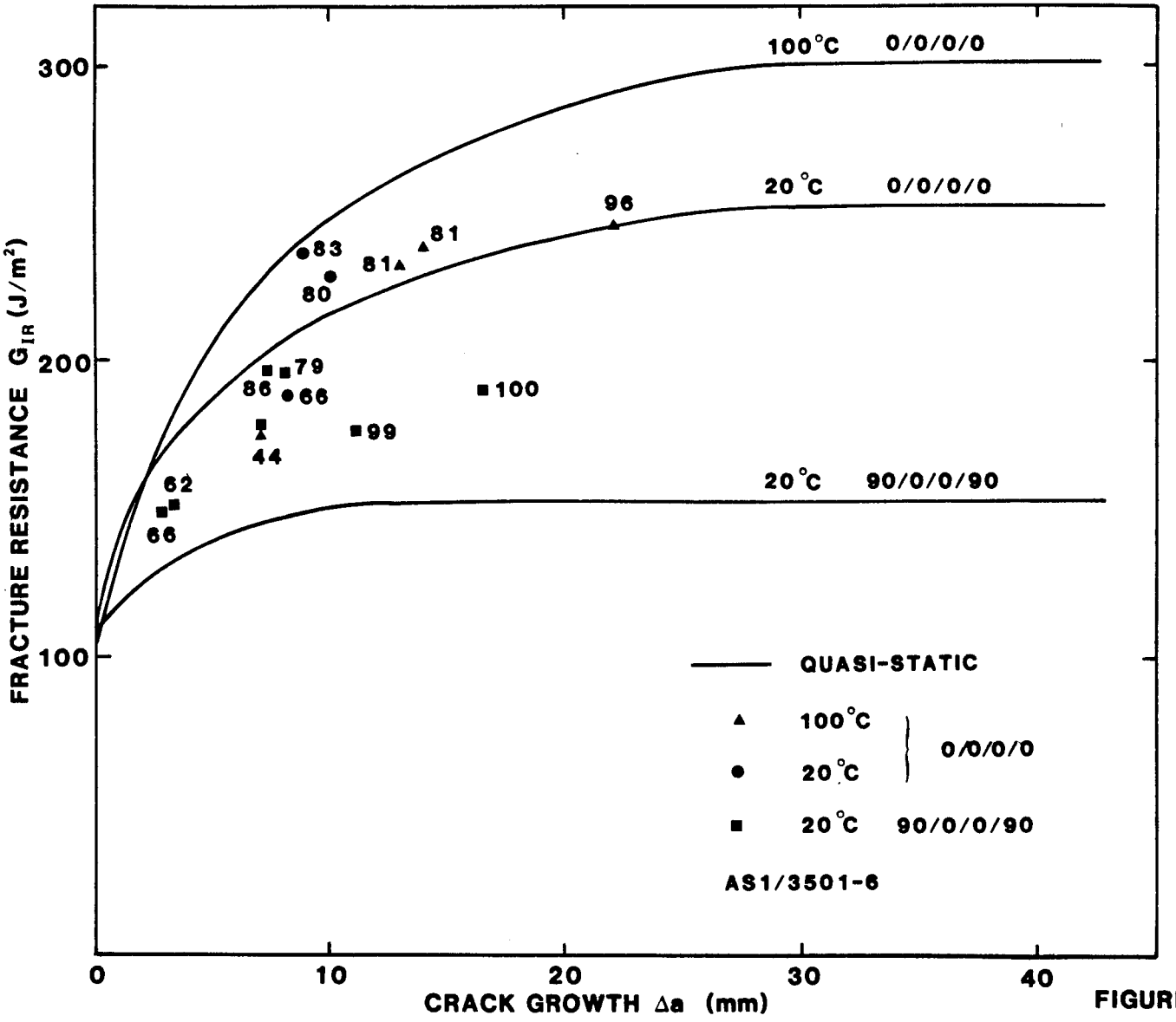
100°C 0/0/0/0
20°C 0/0/0/0
20°C 90/0/0/90
FRACTURE RESISTANCE G_{IR} (J/m²)
CRACK GROWTH Δa (mm)
300
200
100
0
10
20
30
40
83
80
81
81
96
79
86
66
100
99
44
62
66
QUASI-STATIC
100°C
20°C
0/0/0/0
20°C 90/0/0/90
AS1/3501-6

FIGURE 8

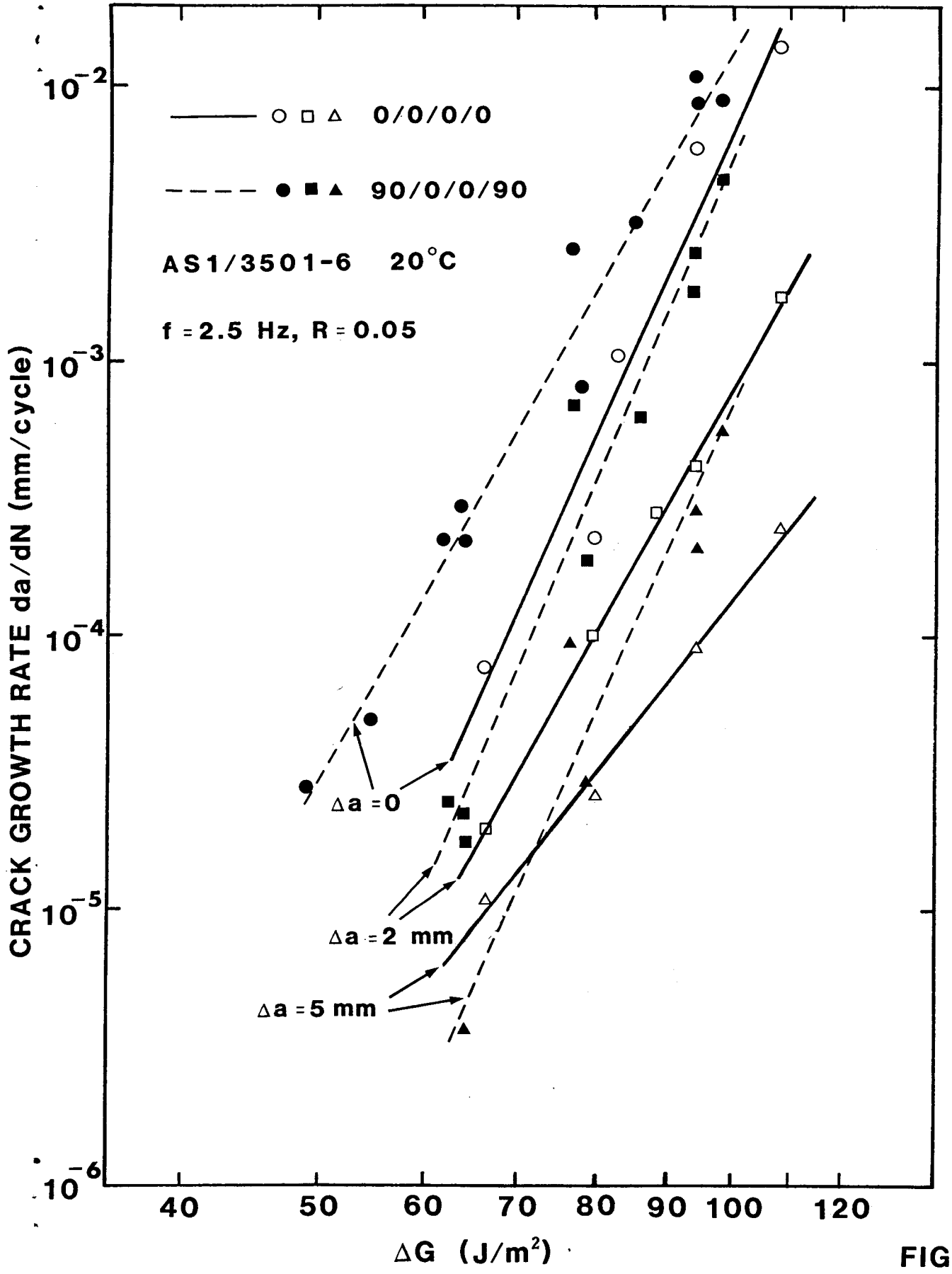
0/0/0/0
90/0/0/90
AS1/3501-6 20°C
f = 2.5 Hz, R = 0.05
Δa = 0
Δa = 2 mm
Δa = 5 mm
CRACK GROWTH RATE da/dN (mm/cycle)
ΔG (J/m²)
10⁻²
10⁻³
10⁻⁴
10⁻⁵
10⁻⁶
40
50
60
70
80
90
100
120

FIGURE 9

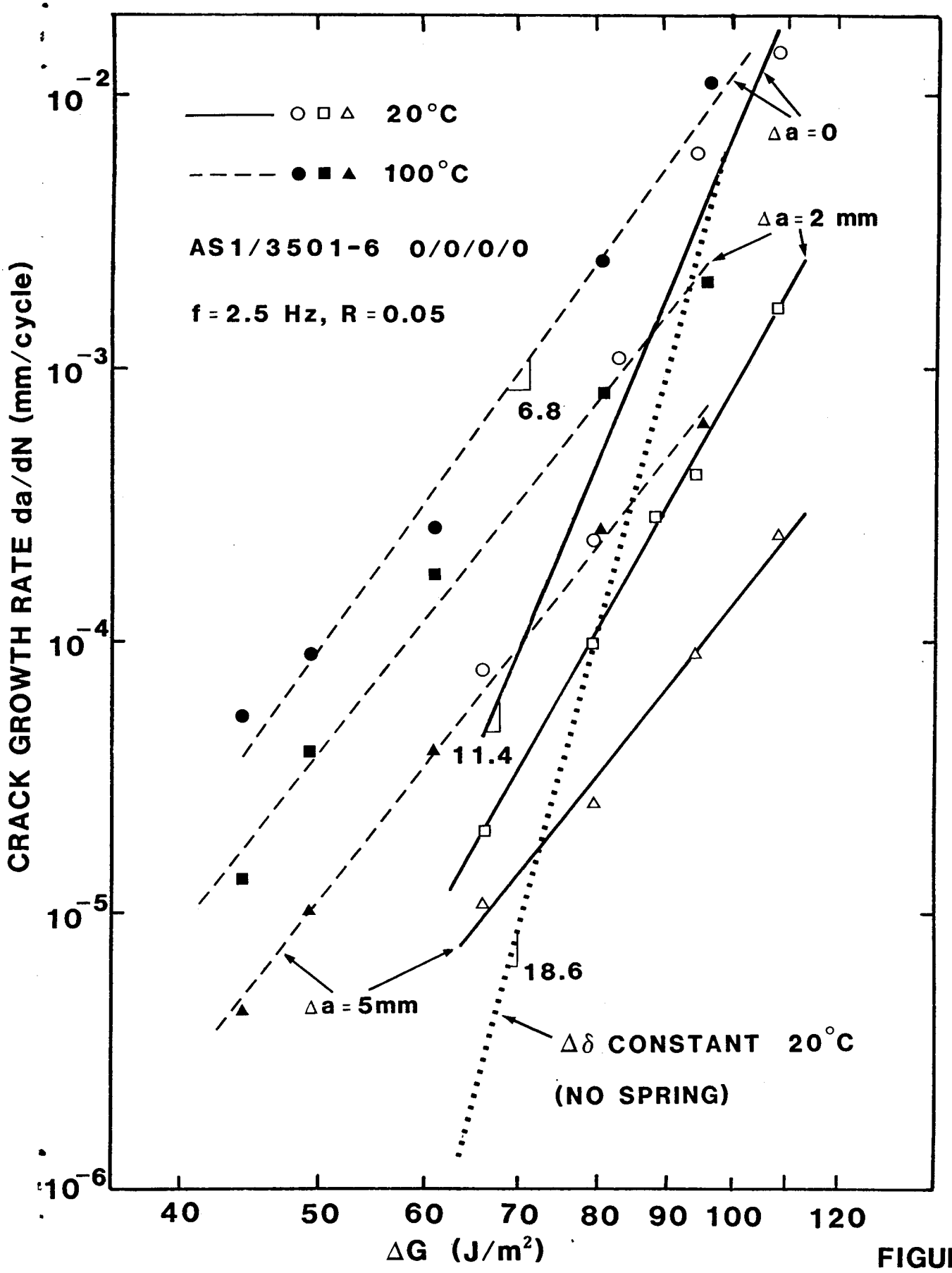
CRACK GROWTH RATE da/dN (mm/cycle)
10^{-2}
10^{-3}
10^{-4}
10^{-5}
10^{-6}
20°C
100°C
AS1/3501-6 0/0/0/0
f = 2.5 Hz, R = 0.05
Δa = 0
Δa = 2 mm
Δa = 5mm
6.8
11.4
18.6
Δδ CONSTANT 20°C
(NO SPRING)
40
50
60
70
80
90
100
120
ΔG (J/m²)

FIGURE 10

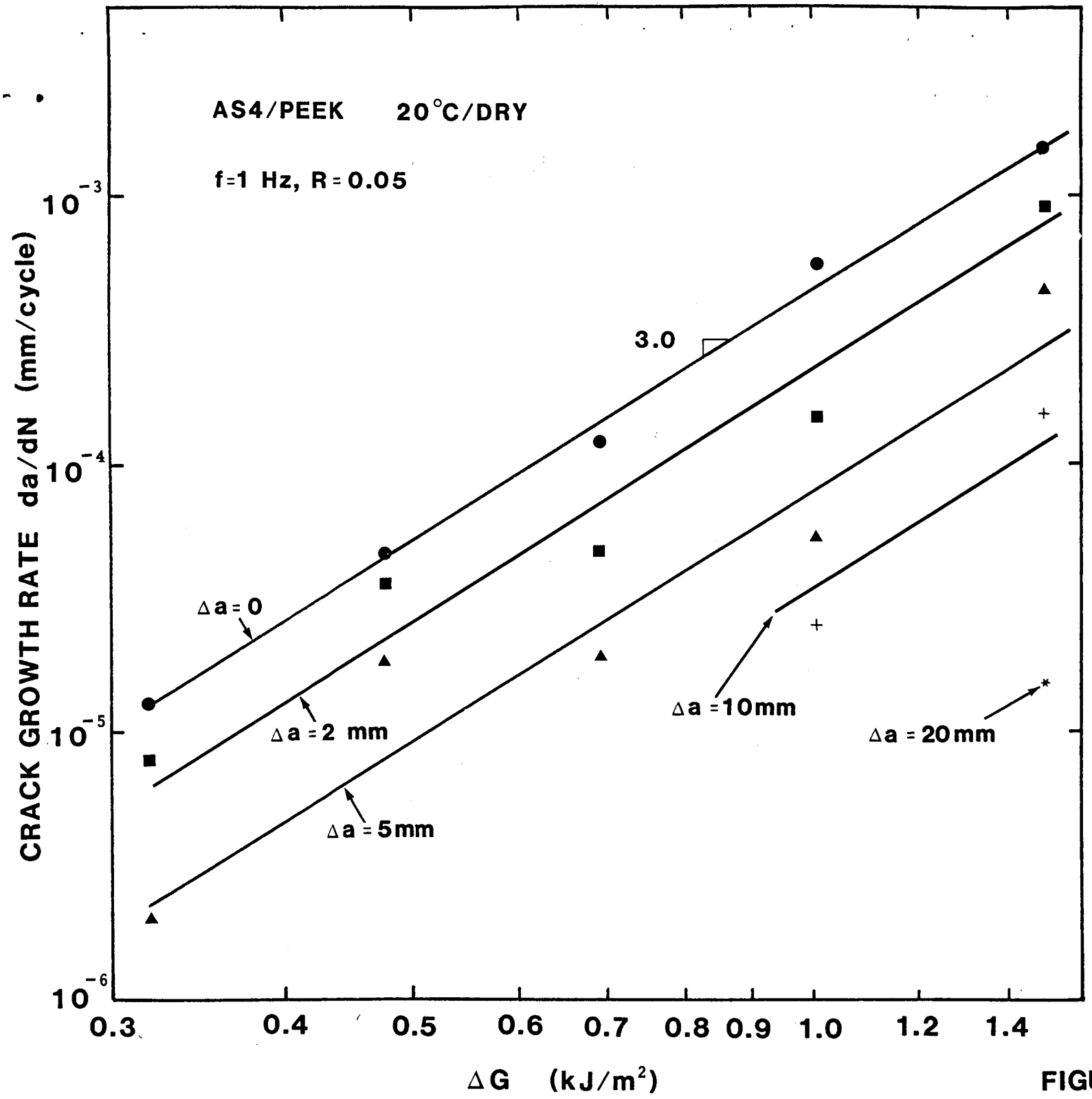
AS4/PEEK 20°C/DRY
f=1 Hz, R=0.05
CRACK GROWTH RATE da/dN (mm/cycle)
10^{-3}
10^{-4}
10^{-5}
10^{-6}
3.0
Δa = 0
Δa = 2 mm
Δa = 5mm
Δa = 10mm
Δa = 20mm
0.3
0.4
0.5
0.6
0.7
0.8
0.9
1.0
1.2
1.4
ΔG (kJ/m²)

FIGURE 11

CRACK GROWTH DIRECTION

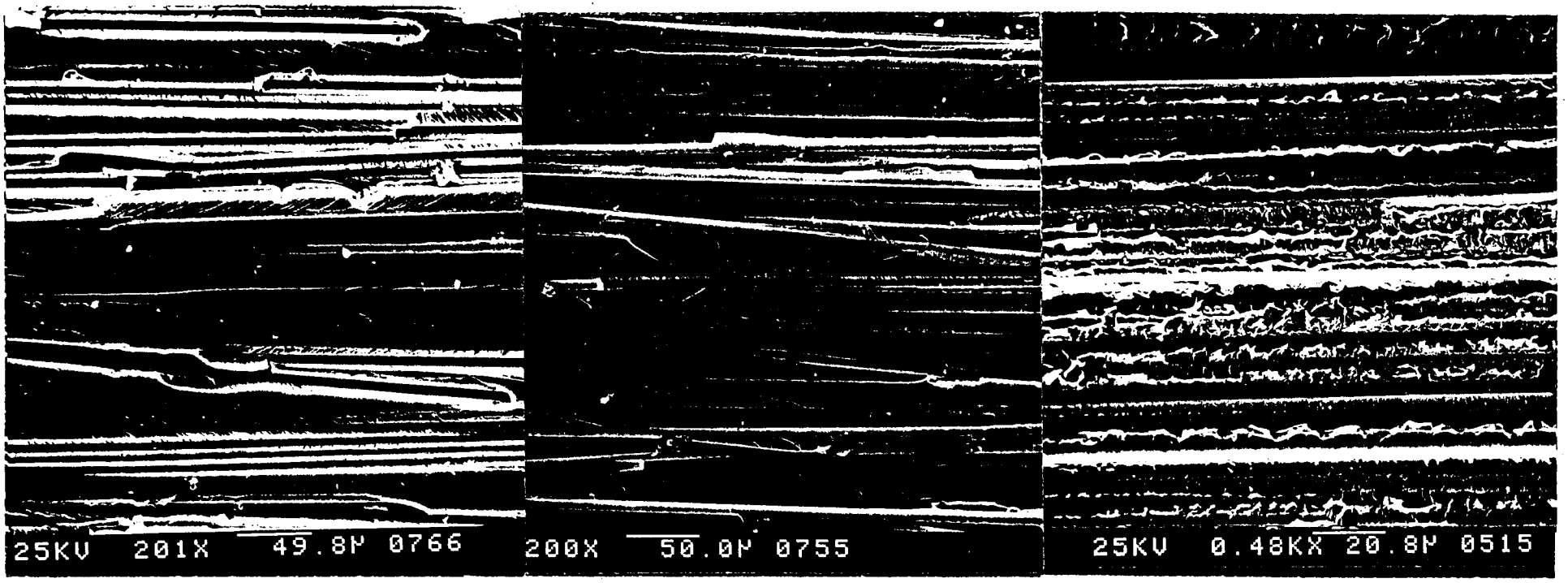

90/0/0/90 $\Delta G = 62$ J/m^2 0/0/0/0 $\Delta G = 66$ J/m^2 0/0/0/0 $\Delta G = 1495$ J/m^2

AS1/3501-6 AS4/PEEK

FIGURE 12

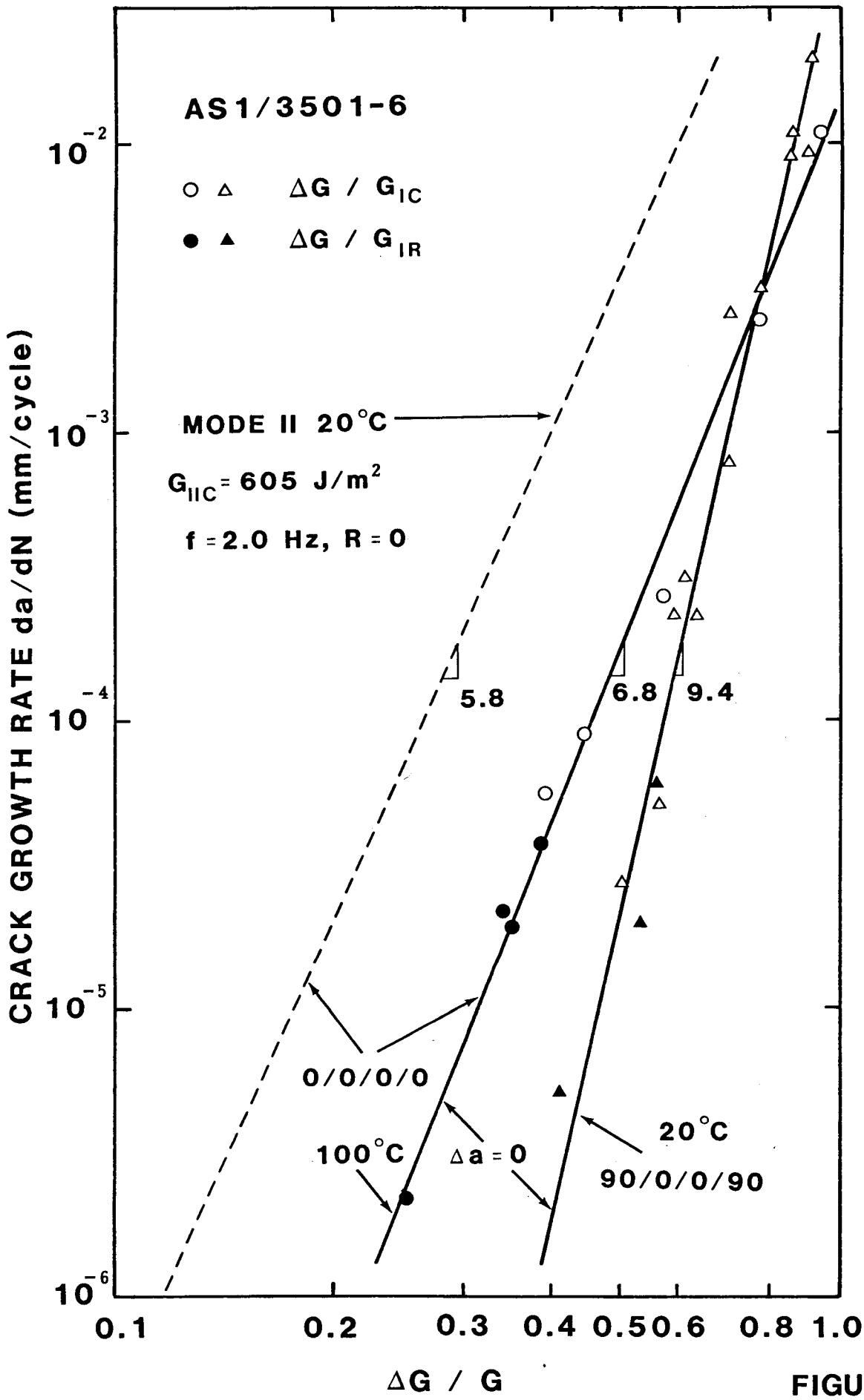
AS1/3501-6
○ △ ΔG / G_IC
● ▲ ΔG / G_IR
MODE II 20°C
G_IIC = 605 J/m²
f = 2.0 Hz, R = 0
5.8
6.8
9.4
0/0/0/0
100°C
Δa = 0
20°C
90/0/0/90
CRACK GROWTH RATE da/dN (mm/cycle)
10⁻²
10⁻³
10⁻⁴
10⁻⁵
10⁻⁶
0.1
0.2
0.3
0.4
0.5
0.6
0.8
1.0
ΔG / G

FIGURE 13

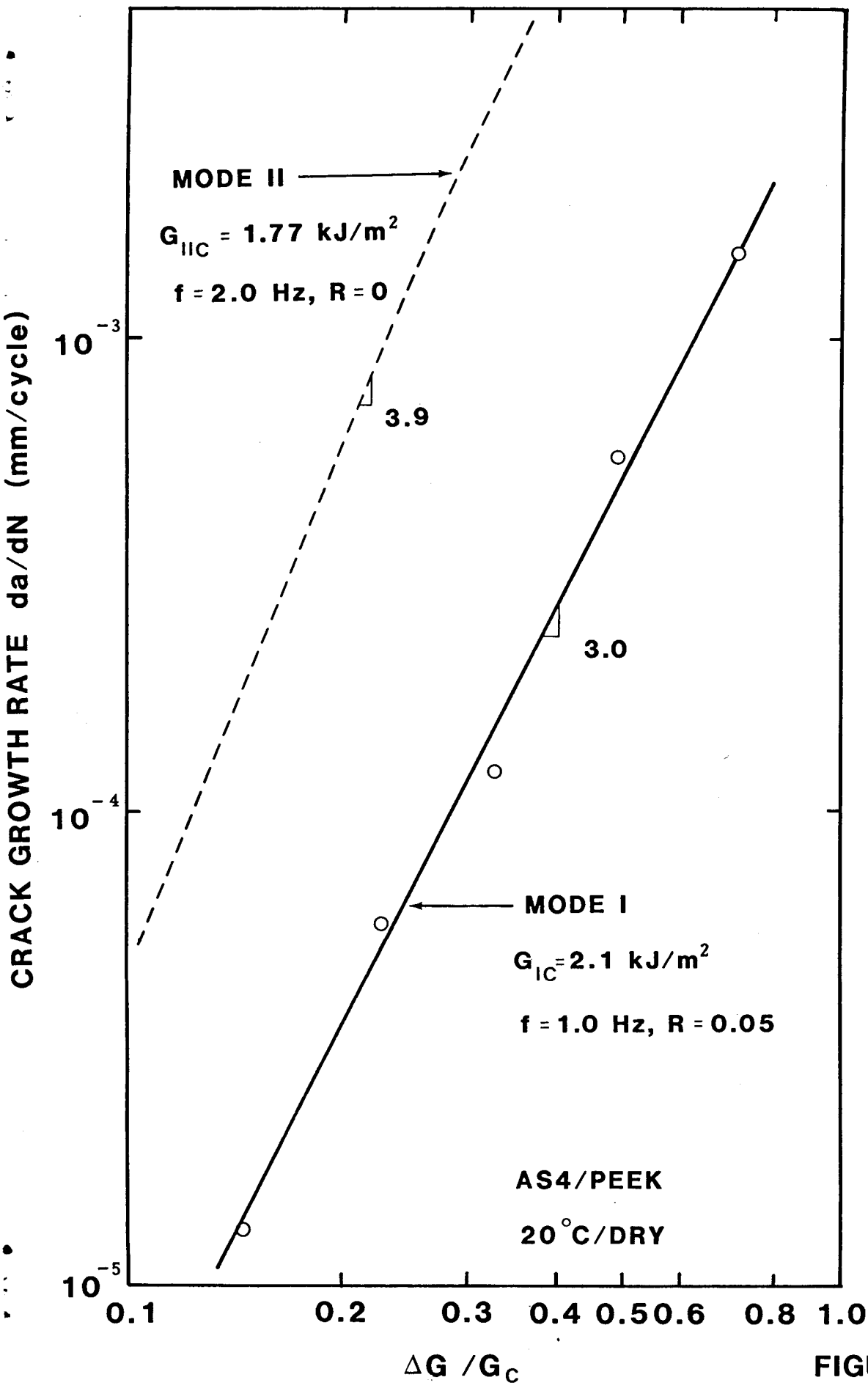
MODE II
G_{IIC} = 1.77 kJ/m^2
f = 2.0 Hz, R = 0
3.9
3.0
MODE I
G_{IC}=2.1 kJ/m^2
f = 1.0 Hz, R = 0.05
AS4/PEEK
20°C/DRY
CRACK GROWTH RATE da/dN (mm/cycle)
10^{-3}
10^{-4}
10^{-5}
0.1
0.2
0.3
0.4
0.5
0.6
0.8
1.0
$\Delta G / G_C$

FIGURE 14